Hindawi
Advances in Civil Engineering
Volume 2020, Article ID 4292043, 11 pages
https://doi.org/10.1155/2020/4292043

Research Article

Visco-Elastoplastic Constitutive Fatigue Model for Rocks

Jianhao Liu,[1] Shaoyun Pu ,[1,2] and Junying Rao[1]

[1]*School of Civil Engineering, Guizhou University, Guiyang, Guizhou 550025, China*
[2]*School of Transportation, Southeast University, Nanjing, Jiangsu 211189, China*

Correspondence should be addressed to Shaoyun Pu; pushaoyun@seu.edu.cn

Received 10 August 2019; Revised 20 May 2020; Accepted 26 May 2020; Published 11 June 2020

Academic Editor: Eric M. Lui

The study on the constitutive fatigue model for rocks under cyclic loading has an important significance in rock engineering. In order to study the fatigue properties of rocks under cyclic loading, according to the theory of rheological mechanics and the existing three basic one-dimensional fatigue elements, i.e., elastic, viscous, and plastic fatigue elements, the three-dimensional elastic, viscous, and plastic fatigue elements were constructed. Meanwhile, a fatigue yield criterion for rocks under cyclic loading was proposed, and a three-dimensional nonlinear visco-elastoplastic fatigue constitutive model (NVPFM) for rocks was established by using the flow criterion related to the proposed fatigue yield criterion. Compared with the test results of rocks under cyclic loading, the three-dimensional NVPFM could be used to describe the transient, steady-state, and tertiary creep phases of rocks under cyclic loading.

1. Introduction

When rocks are subjected to cyclic or dynamic loading, different types of rocks have different responses. Some rocks may become stronger under cyclic loading, while others become more fragile [1]. In geotechnical engineering, fatigue problems are often involved such as coal walls under mining stress [2–5], side slope of the dam under cyclic variation water level [6], tunnels under traffic loading, and the surrounding rocks under earthquake load [7–12]. The strength of rocks under long-term cyclic loading will be reduced; thus, fatigue damage of rocks is caused, and the engineering accidents may be caused. Therefore, the study of fatigue characteristics of rocks under cyclic loading is of theoretical significance for the long-term stability evaluation and design of geotechnical engineering.

For rocks under long-term cyclic loading, even if the upper limit of cyclic loading is lower than the static strength of the material, the material can also be destroyed; this phenomenon is called fatigue [13]. There is no exception for rocks [14–17]. The mechanical properties of rocks under cyclic loading are more complex than those under static load. The mechanical properties of rocks under cyclic loading are affected by many factors. The fatigue life of rocks is related to the stress amplitude of cyclic loading [18–21], and the dynamic strength of rocks is related to the stress amplitude of cyclic loading and the stress upper limit of cyclic loading. Similarly, the dynamic strength of rocks is also affected by loading rate and the frequency of cyclic loading [22–29]. There is a threshold value for rocks under cyclic loading, also known as critical strength. The deformation of rocks under cyclic loading is similar to the creep of rocks under static load [30]. When the upper limit of cyclic loading is higher than the critical strength, fatigue failure will occur [31–33]. However, when the upper limit of cyclic loading is less than the critical strength, fatigue failure does not occur. In order to study the fatigue deformation characteristics of rocks under cyclic loading, some scholars studied the damage process of rocks from the perspective of damage mechanics. The damage of rocks under cyclic loading is divided into three stages [34]. Xiao et al. proposed an inverted-*S* damage model to describe the damage process of rocks under cyclic loading [35, 36]. Meanwhile, there are many constitutive models based on damage theory [37–39]. Additionally, internal variable fatigue constitutive model of rocks was also proposed [40]. However, in recent years, the component model based on rheological mechanics has been applied to build the constitutive model of rocks under cyclic

loading as well. Wang et al. [41] established a burgers fatigue model under cyclic confining stress loading with low cyclic frequency. Guo and Huang [42] proposed three one-dimensional fatigue elements, i.e., elastic fatigue element, viscous fatigue element, and plastic fatigue element, and used creep theory to establish a nonlinear fatigue constitutive model of rocks under uniaxial cyclic loading by simplifying the cyclic loading reasonably.

The research on the fatigue constitutive model for rocks is mainly based on the damage theory. Although the established constitutive models can effectively describe the rock fatigue deformation characteristic, most of the proposed models can only reflect the fatigue properties of rocks under uniaxial conditions. Moreover, some proposed models cannot reflect the influence of the properties of cyclic loading and strength of rocks on fatigue deformation of rocks. However, at present, the study of the three-dimensional fatigue constitutive model for rocks under cyclic loading is still lacking. Consequently, in this article, on the basis of rheological mechanics and the previous study [42], three three-dimensional fatigue elements, i.e., elastic, viscous, and plastic elements, are constructed. Moreover, the fatigue yield criterion for rocks under cyclic loading was proposed, and a three-dimensional nonlinear viscoelastic-plastic fatigue model was established using the flow criterion related to the fatigue yield criterion. The rock fatigue constitutive equations under triaxial conditions were deduced. Finally, the model parameters were identified, and model applicability was verified.

2. Basic Theory of Rock Fatigue

2.1. Cyclic Loading. The common types of cyclic loading are sinusoidal wave, cosine wave, rectangular wave, and triangular wave cyclic loading. The cyclic loading can be expressed as

$$\sigma = \sigma\left(\sigma_{\max}, \sigma_{\min}, t, f, A\right), \tag{1}$$

where $\sigma_{\max}$ is the upper limit of cyclic loading; $\sigma_{\min}$ is the lower limit of cyclic loading; f is the frequency of cyclic loading, $f = 1/T$; T is the period of cyclic loading; t is the time of cyclic loading, and the relationship between N and t is $t = NT$; N is a positive integer; and A is the stress amplitude of cyclic loading.

2.2. Fatigue Behavior of Rocks. When the upper limit of cyclic loading is higher than the critical strength, fatigue failure will occur, and the creep behavior presents transient, steady-state, and tertiary creep phases (see II curve in Figures 1(a) and 1(b)) [30–33, 44]. The creep phases of under cyclic loading are also called as deceleration, constant velocity, and acceleration creep. However, when the upper limit of cyclic loading is less than the critical strength, fatigue failure does not occur, and the creep behavior presents two creep stages, i.e., transient and steady-state (see I curve in Figure 1(a)) [43, 45].

2.3. Simplified Cyclic Loading. To use the component model based on rheological mechanics, assume that σ_1 is the direction of the cyclic loading and it is the first principal stress. Under confining pressure, the equivalent deviatoric stress acting on rocks under cyclic loading was simplified into the following stress function in our previous study [46]:

$$\sigma_1 - \sigma_3 = \sigma_{\text{av}} \exp\left\{\left[\frac{(\sigma_{1\max} - \sigma_3) - \sigma_s}{\sigma_c}\right] f\right\}, \tag{2}$$

where σ_{av} is the average stress of cyclic loading, $\sigma_1(t) - \sigma_3$; $\sigma_{1\max}$ is the upper limit of cyclic loading; σ_s is the critical strength of the rock under the complex stress state, which is the maximum stress value from the $(\sigma_1 - \sigma_3) - \varepsilon$ curve of the rock under cyclic loading when the rock happens to be destroyed; σ_c is the peak stress from the $(\sigma_1 - \sigma_3) - \varepsilon$ curve of the rock under static load; and σ_3 is the small principal stress on rock specimens.

According to equation (2), when the peak deviatoric stress of cyclic loading $(\sigma_{1\max} - \sigma_3) > \sigma_s$, the equivalent deviatoric stress $(\sigma_1 - \sigma_3) > \sigma_{\text{av}}$, and the fatigue breakdown of the rock will occur. When the peak deviatoric stress of cyclic loading $(\sigma_{1\max} - \sigma_3) \le \sigma_s$, the equivalent deviatoric stress $(\sigma_1 - \sigma_3) \le \sigma_{\text{av}}$, and the rocks do not undergo fatigue breakdown.

When confining pressure $\sigma_3 = 0$, the cyclic loading is simplified into the stress function shown in the following equation [42]:

$$\sigma = \sigma_{\text{av}} \exp\left[\left(\frac{\sigma_{\max} - \sigma_s}{\sigma_c}\right) f\right], \tag{3}$$

where σ_{av} is the average stress of cyclic loading; $\sigma_{\max}$ is the upper limit of cyclic loading; σ_s is the critical strength of the rock under uniaxial cyclic loading; and σ_c is the rock uniaxial compressive strength.

Similarly, according to equation (3), when $\sigma_{\max} > \sigma_s$, the simplified stress $\sigma > \sigma_{\text{av}}$, and the rock will undergo fatigue breakdown. However, when $\sigma_{\max} \le \sigma_s$, $\sigma \le \sigma_{\text{av}}$, and the rock does not undergo fatigue breakdown.

2.4. Fatigue Yield Criterion for Rocks

2.4.1. Rock Fatigue Yield Criterion under Uniaxial Stress. Under uniaxial cyclic loading, when $\sigma_{\max} \le \sigma_s$, namely, $\sigma \le \sigma_{\text{av}}$, the rock will undergo fatigue damage. When $\sigma_{\max} \le \sigma_s$, $\sigma \le \sigma_{\text{av}}$, and the rock will not undergo fatigue failure.

2.4.2. Rock Fatigue Yield Criterion under Confining Pressure. Regardless of the effect of spherical stress tensor on fatigue deformation, it is assumed that fatigue deformation of the rock is related only to the second invariant of stress deviator J_2. According to equation (2), the proposed fatigue yield criterion of the rock under cyclic loading is as follows:

$$F\left(J_2, \sigma_{\text{av}}\right) = \sqrt{J_2} - \frac{\sigma_{\text{av}}}{\sqrt{3}}, \tag{4}$$

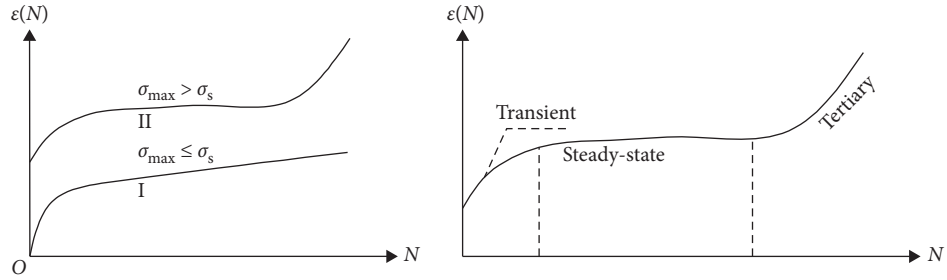

Figure 1: Typical creep characteristics of the rock under cyclic loading [43]. (a) Creep curves of the rock under cyclic loading. (b) Division of creep stages.

where J_2 is the second invariant of the equivalent stress deviator, $J_2 = \sqrt{1/6[(\sigma_1 - \sigma_2)^2 + (\sigma_2 - \sigma_3)^2 + (\sigma_3 - \sigma_1)^2]}$.

When $\sigma_2 = \sigma_3$, $F(J_2, \sigma_{av}) = (\sigma_1 - \sigma_3 - \sigma_{av})/\sqrt{3}$. When $(\sigma_1 - \sigma_3) > \sigma_{av}$, $F(J_2, \sigma_{av}) > 0$, and the rock will undergo fatigue breakdown. Conversely, when $(\sigma_1 - \sigma_3) < \sigma_{av}$, $F(J_2, \sigma_{av}) < 0$, and the rock does not undergo fatigue breakdown. Consequently, the established equation (4) can be used as a fatigue yield function for rocks under cyclic loading, and the yield criterion is a function of σ_{av} of cyclic loading and equivalent stress.

2.5. Basic One-Dimensional Fatigue Elements [42]. The one-dimensional fatigue model consists of three basic fatigue elements [42], i.e., elastic, viscous, and plastic fatigue elements. For the elastic fatigue element (see Figure 2(a)), the stress acting on the material is proportional to the strain. For the viscous fatigue element (see Figure 2(b)), the stress acting on the material is proportional to the strain rate. The plastic fatigue element is represented by friction sheets shown in Figure 2(c). The constitutive equations are as follows:

2.5.1. Elastic Fatigue Element [42].

$$\sigma = E\varepsilon^e(N), \tag{5}$$

where E is the elastic fatigue coefficient, which can be determined by the numerical fitting method. $\varepsilon^e(N)$ is the fatigue strain.

2.5.2. Viscous Fatigue Element [42].

$$\sigma = \eta \frac{d\varepsilon^v(t)}{dt} = \eta \frac{d\varepsilon^v(N)}{dN} f, \tag{6}$$

where η is the viscous fatigue coefficient, which can be determined by the numerical method, $d\varepsilon^v(t)/dt$ is the strain increment of the viscous fatigue element within the time period $[t, t + \Delta t]$, and $d\varepsilon^v(N)/dt$ is the fatigue strain increment of the element in each cycle of cyclic loading.

2.5.3. Plastic Fatigue Element [42]. When $\sigma_{max} \le \sigma_s$, that is, $\sigma \le \sigma_{av}$, even if the cycle number N tends to infinity, the fatigue strain of the element is still 0. When $\sigma_{max} \le \sigma_s$, namely, $\sigma \le \sigma_{av}$, rocks will undergo fatigue breakdown, and the fatigue strain of rocks will continue to increase with the increase in the number of cycles of cyclic loading . The equation of the state of the plastic fatigue element is

$$\begin{cases} \varepsilon^p(N) \longrightarrow \infty, & \sigma_s > \sigma_{max}, \text{ namely}, \sigma > \sigma_{av}, \\ \varepsilon^p(N) = 0, & \sigma_s \le \sigma_{max}, \text{ namely}, \sigma \le \sigma_{av}, \end{cases} \tag{7}$$

where $\varepsilon^p(N)$ is the plastic strain of the plastic fatigue element.

Based on the above establishment process of one-dimensional fatigue elements and rheological mechanics theory, the three-dimensional fatigue elements under confining pressure can be established in this article.

2.6. Establishment of Three-Dimensional Fatigue Elements

2.6.1. Three-Dimensional (3D) Elastic Fatigue Element. The three-dimensional elastic fatigue element is shown in Figure 3, and its equation of state is

$$\begin{cases} S_{ij} = 2G_1 e^e_{ij}(N), \\ \varepsilon_{kk} = \dfrac{1}{3K}\sigma_{kk}, \end{cases} \tag{8}$$

where S_{ij} is the equivalent deviatoric stress tensor $S_{ij} = \sigma_{ij} - \sigma_m \delta_{ij}$, in which δ_{ij} is the Kronecker delta; $e^e_{ij}(N)$ is the deviatoric strain tensor of the fatigue element; σ_{kk} is the first invariant of the stress tensor; ε_{kk} is the first invariant of the strain tensor; and K is the fatigue volume modulus of the rock, and its physical dimension is stress.

Then, the total strain ε^e_{ij} of the 3D elastic fatigue element under σ_{ij} is

$$\varepsilon^e_{ij} = \frac{1}{2G_1} S_{ij} + \frac{1}{3K}\sigma_m \delta_{ij} = \frac{1}{2G_1} S_{ij} + \frac{1}{9K}\sigma_{kk}\delta_{ij}, \tag{9}$$

where $\sigma_m \delta_{ij}$ is the spherical stress tensor, $\sigma_m = \sigma_{kk}/3$.

2.6.2. Three-Dimensional (3D) Viscous Fatigue Element. For the 3D viscous fatigue element (see Figure 4), without considering the volume strain of the element under the spherical stress tensor, the state equation of the element is

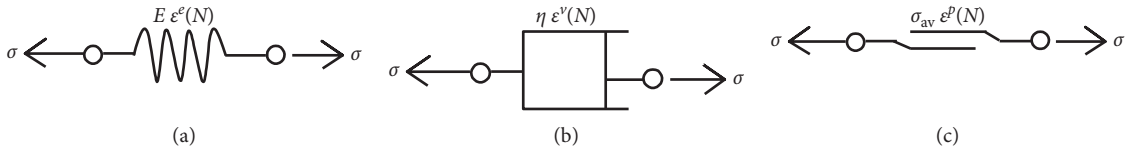

Figure 2: One-dimensional fatigue element [42].

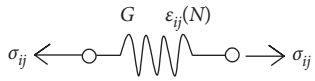

Figure 3: 3D elastic fatigue element.

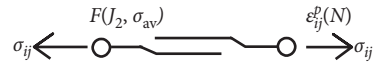

Figure 5: 3D plastic fatigue element.

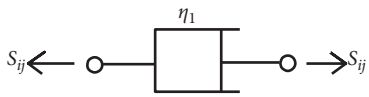

Figure 4: 3D viscous fatigue element.

$$S_{ij} = 2\eta_1 \dot{e}^{v}_{ij}(t) = 2f\eta_1 \dot{e}^{v}_{ij}(N), \tag{10}$$

where $\dot{e}^{v}_{ij}(t)$ is the increment of the deviatoric strain of the fatigue element in period $[t, t+\Delta t]$ and $\dot{e}^{v}_{ij}(N)$ is the deviatoric strain increment of the viscous fatigue element in each cycle.

The following equation can be obtained by integrating equation (10):

$$e^{v}_{ij}(N) = \frac{1}{2\eta_1}\left(\frac{N}{f}\right)S_{ij}, \tag{11}$$

where $e^{v}_{ij}(N)$ is the deviatoric strain of the viscous fatigue element.

2.6.3. Three-Dimensional (3D) Plastic Fatigue Element. Three-dimensional plastic fatigue element can be represented by the friction sheet shown in Figure 5. When $\sigma_{\max} - \sigma_3 \le \sigma_s$, namely, $F(J_2, \sigma_{av}) \le 0$, and even if the number of cycles N tends to infinity, the element fatigue strain is still 0. When $\sigma_{\max} - \sigma_3 > \sigma_s$, namely, $F(J_2, \sigma_{av}) > 0$, fatigue failure can occur in rocks, and the fatigue strain of rocks will still increase with the increase in the number of cycles of cyclic loading. The equation of state of the element is

$$\begin{cases} \varepsilon^{p}_{ij}(N) \longrightarrow \infty, & \sigma_{\max} - \sigma_3 > \sigma_s \text{ or } F(J_2, \sigma_{av}) > 0, \\ \varepsilon^{p}_{ij}(N) = 0, & \sigma_{\max} - \sigma_3 \le \sigma_s \text{ or } F(J_2, \sigma_{av}) \le 0, \end{cases} \tag{12}$$

where $\varepsilon^{p}_{ij}(N)$ is the plastic strain of the plastic fatigue element.

3. Three-Dimensional Nonlinear Visco-Elastoplastic Fatigue Constitutive Model for Rocks

The Burgers fatigue model consists of a series of Maxwell and Kelvin fatigue models, which can describe the transient and steady-state creep phases of the rock but cannot describe the tertiary creep phases of the rock. To fully describe the law of creep of the rock under cyclic loading, a nonlinear visco-elastoplastic fatigue model is connected to the burgers model in series, which is a one-dimensional nonlinear visco-elastoplastic fatigue constitutive model (see Figure 6) proposed by Guo and Huang [42].

Schiessel et al. [47] considered the time accumulation of the viscous elements (η_K) in the Kelvin body and defined the fractional viscous element by fractional derivatives. The creep compliance $J(t)$ of the fractional element is proportional to t^{β}; β is a constant, and t is the rheological time. According to the aforementioned and Guo and Huang's study [42], the viscous coefficient of the series-connected viscous fatigue element in the nonlinear visco-elastoplastic fatigue model, shown in Figure 6, is

$$\eta_3(t, n) = \eta_{30} t^{1-n}, \tag{13}$$

where n is the parameter that reflects the strain rate of the tertiary creep phases of the rock under cyclic loading, $n \ne 1$. η_{30} is the initial value of the viscous coefficient, and $\eta_{30} \ne 0$; its physical dimension is stress·time n. Equation (13) can also be further expressed as

$$\eta_3(N) = \eta_{30}(N/f)^{1-n}. \tag{14}$$

3.1. Establishment of the Nonlinear Viscoplastic Fatigue Model. Under confining pressure stress, the fatigue mechanics parameters of the rock are different from those under one-dimensional stress. The three-dimensional nonlinear viscoelastic-plastic fatigue model consists of a three-dimensional elastic fatigue element, a viscous fatigue element, a viscoelastic fatigue model, and a nonlinear viscoplastic fatigue model (see Figure 7). In the model, G_1 is the elastic shear fatigue coefficient, G_2 is the viscoelastic shear fatigue coefficient, η_1 is the viscous shear fatigue coefficient, η_2 is the viscoplastic shear fatigue coefficient, and η_{30} is the initial value of the viscoplastic shear fatigue coefficient. The physical dimension of model parameters G_1 and G_2 is stress.

3.2. Viscoelastic Fatigue Model. For the viscoelastic fatigue model shown in Figure 8, the effect of the spherical stress tensor on volumetric strain is not considered. The state

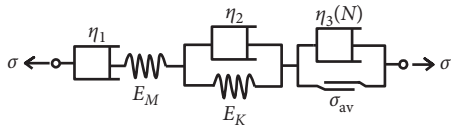

Figure 6: One-dimensional NVPFM of the rock [42].

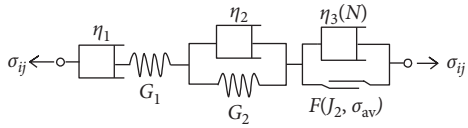

Figure 7: Three-dimensional NVPFM for the rock.

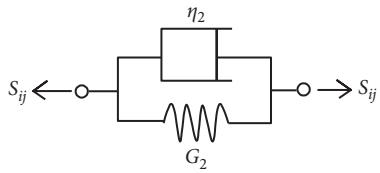

Figure 8: Three-dimensional viscoelastic fatigue model.

equation of the viscoelastic fatigue model, shown in Figure 8, is

$$S_{ij} = 2G_2 e_{ij}^{ve}(t) + 2\eta_2 \dot{e}_{ij}^{ve}(t) = 2G_2 e_{ij}^{ve}(N) + 2f\eta_2 \dot{e}_{ij}^{ve}(N), \tag{15}$$

where $\dot{e}_{ij}^{ve}(t)$ is the deviator strain increment of the fatigue element in the time period $[t, t+\Delta t]$, $\dot{e}_{ij}^{v}(N)$ is the deviator strain increment of the fatigue element in each cycle, and $e_{ij}^{ve}(N)$ is the deviator strain tensor of the fatigue element.

The following fatigue constitutive equation of the fatigue element can be obtained from equation (15):

$$e_{ij}^{ve}(N) = \frac{1}{2G_2}\left\{1 - \exp\left[-\frac{G_2}{\eta_2}\left(\frac{N}{f}\right)\right]\right\} S_{ij}. \tag{16}$$

3.3. Nonlinear Viscoplastic Fatigue Model. For the viscoplastic fatigue model shown in Figure 9, the viscoplastic shear fatigue coefficient $\eta_3(N)$ in the model is the same as equation (14), and the plastic strain rate of the fatigue model according to the rheologic basic principle can be written as

$$\dot{e}_{ij}^{nl}(t) = f\dot{e}_{ij}^{nl}(N) = \frac{1}{\eta_3(N)}\varphi(F)\frac{\partial Q}{\partial \sigma_{ij}}, \tag{17}$$

where $\dot{e}_{ij}^{nl}(t)$ is the deviator strain increment of the fatigue element in the time period $[t, t+\Delta t]$; $\dot{e}_{ij}^{nl}(N)$ is the deviator strain increment of the fatigue element in each cycle; F is the fatigue yield function of the rock; and Q is the plastic potential function of rock fatigue.

The following fatigue constitutive equation can be obtained by substituting equation (14) into equation (17) and integrating N:

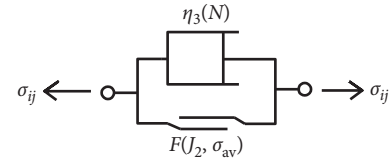

Figure 9: Three-dimensional nonlinear viscoplastic fatigue model.

$$e_{ij}^{nl}(N) = \frac{1}{\eta_{30} n}\varphi(F)\frac{\partial Q}{\partial \sigma_{ij}}\left(\frac{N}{f}\right)^n, \tag{18}$$

where $e_{ij}^{nl}(N)$ is the plastic deviator strain tensor of the nonlinear viscoplastic fatigue model. Among them,

$$\langle \varphi(F) \rangle = \begin{cases} 0, & (F < 0), \\ \varphi(F), & (F > 0), \end{cases} \tag{19}$$

$$\varphi(F) = \sum_{m=1}^{M} B_m F^m. \tag{20}$$

In equation (20) [48], B_m, m, and M are constants. In this article, we used $M = 1$ and $B_1 = 1$ for convenience.

When $F(J_2, \sigma_{av}) \le 0$, the rock does not undergo fatigue breakdown. When $F(J_2, \sigma_{av}) > 0$, the following fatigue constitutive equation of the fatigue element can be obtained by using the flow rules related to the fatigue yield criterion:

$$e_{ij}^{nl}(N) = \frac{1}{\eta_{30} n} F \frac{\partial F}{\partial \sigma_{ij}}\left(\frac{N}{f}\right)^n. \tag{21}$$

3.4. Constitutive Equation of the Nonlinear Visco-Elastoplastic Fatigue Model. When the rock fatigue yield function $F(J_2, \sigma_{av}) \le 0$, the rock will not be subjected to fatigue failure. At this time, the model degenerates into a burgers model which can describe the two creep stages of the rock under cyclic loading, i.e., transient and steady-state phases. From equations (8)–(20), the constitutive equation of the fatigue model can be obtained as

$$\begin{aligned} \varepsilon_{ij}(N) = {} & \frac{1}{2G_1} S_{ij} + \frac{1}{3K}\sigma_m \delta_{ij} + \frac{\sigma}{2\eta_1}\left(\frac{N}{f}\right) S_{ij} \\ & + \frac{1}{2G_2}\left\{1 - \exp\left[-\frac{G_2}{\eta_2}\left(\frac{N}{f}\right)\right]\right\} S_{ij}, \end{aligned} \tag{22}$$

where $\varepsilon_{ij}(N)$ is the total strain tensor of the fatigue model.

When the rock fatigue yield function $F(J_2, \sigma_{av}) > 0$, the rock will undergo fatigue failure. At this time, the model is a 3D nonlinear visco-elastoplastic fatigue model which can describe the three creep stages of the rock under cyclic loading, i.e., transient, steady-state, and tertiary creep phases. From equations (8)–(21), the following constitutive equation of the fatigue model can be obtained:

$$\varepsilon_{ij}(N) = \frac{1}{2G_1}S_{ij} + \frac{\sigma}{2\eta_1}\left(\frac{N}{f}\right)S_{ij} + \frac{1}{2G_2}\left\{1 - \exp\left[-\frac{G_2}{\eta_2}\left(\frac{N}{f}\right)\right]\right\}S_{ij} + \frac{1}{3K}\sigma_m\delta_{ij} + \frac{1}{\eta_{30}n}F\frac{\partial F}{\partial\sigma_{ij}}\left(\frac{N}{f}\right)^n. \tag{23}$$

4. Fatigue Constitutive Equation for Rocks under Triaxial Compression

The dynamic triaxial test is an indoor method for studying the fatigue properties of rocks under confining pressure stress. The adaptability of the proposed model can be verified by dynamic triaxial test data. Consequently, on the basis of three-dimensional rock fatigue constitutive equation (23), the fatigue constitutive equation under triaxial condition is deduced.

According to equation (2), the equivalent stress state of the rock under dynamic triaxial condition is

$$\sigma_{ij} = \begin{bmatrix} \sigma_1 = \sigma_{\text{av}}\exp\left\{\left[\frac{(\sigma_{1\max} - \sigma_3) - \sigma_s}{\sigma_c}\right]f\right\} + \sigma_3 & 0 & 0 \\ 0 & \sigma_3 & 0 \\ 0 & 0 & \sigma_3 \end{bmatrix}, \quad \sigma_1 > \sigma_3 \geq 0, \tag{24}$$

where σ_3 is the confining pressure acting on specimens.

Deviatoric stress under the simplified stress state is as follows:

$$S_{ij} = \sigma_{ij} - \sigma_m\delta_{ij} = \sigma_{ij} - \frac{1}{3}\sigma_{kk}\delta_{ij}, \tag{25}$$

where δ_{ij} is the Kronecker symbol, σ_{m} is the average stress, $\sigma_m = (\sigma_1 + 2\sigma_3)/3$, and $\sigma_m\delta_{ij}$ is the spherical stress tensor.

The total strain of the rock under dynamic triaxial condition based on the 3D NVPFM is as follows:

$$\varepsilon_{ij}(N) = e_{ij}^e + e_{ij}^v + e_{ij}^{ve} + e_{ij}^{nl} + \frac{1}{3}\left(\varepsilon_v^e + \varepsilon_v^v + \varepsilon_v^{ve} + \varepsilon_v^{nl}\right)\delta_{ij}, \tag{26}$$

where ε_v^e, ε_v^v, ε_v^{ve}, and ε_v^{nl} are rock elastic, viscous, viscoelastic, and viscoplastic volume strains, respectively.

Without considering the viscous, viscoelastic, and viscoplastic volume strains of the rock and considering only the elastic volume strain, then $\varepsilon_v^v = \varepsilon_v^{ve} = \varepsilon_v^{nl} = 0$. Consequently, the following equation can be obtained from equation (26):

$$\varepsilon_{ij}(N) = e_{ij} + \frac{1}{3}\varepsilon_v^e\delta_{ij} = e_{ij} + \frac{1}{3K}\sigma_m\delta_{ij} = e_{ij} + \frac{1}{9K}\sigma_{kk}\delta_{ij}, \tag{27}$$

where e_{ij} is the total deviatoric strain tensor caused by deviatoric stress.

When $F(J_2, \sigma_{\text{av}}) \leq 0$, the rock will not undergo fatigue failure, and circumferential constitutive equation (28) and axial constitutive equation(29) of rocks under dynamic triaxial condition can be obtained by substituting equations (24)–(27) into equation (22):

$$\varepsilon_{11}(N) = \frac{\sigma_1 + 2\sigma_3}{9K} + \frac{\sigma_1 - \sigma_3}{3G_1} + \frac{\sigma_1 - \sigma_3}{3\eta_1}\left(\frac{N}{f}\right) + \frac{1}{3}\frac{\sigma_1 - \sigma_3}{G_2}\left\{1 - \exp\left[-\frac{G_2}{\eta_2}\left(\frac{N}{f}\right)\right]\right\}, \tag{28}$$

$$\varepsilon_{33}(N) = \frac{\sigma_1 + 2\sigma_3}{9K} + \frac{\sigma_3 - \sigma_1}{6G_1} + \frac{\sigma_3 - \sigma_1}{6\eta_1}\left(\frac{N}{f}\right) + \frac{\sigma_3 - \sigma_1}{6G_2}\left(\left\{1 - \exp\left[-\frac{G_2}{\eta_2}\left(\frac{N}{f}\right)\right]\right\}\right). \tag{29}$$

When $F(J_2, \sigma_{\text{av}}) > 0$, the rock will undergo fatigue damage, and circumferential constitutive equation (30) and axial constitutive equation (31) under dynamic triaxial condition can be obtained by substituting equations (24)–(27) into equation (23):

$$\varepsilon_{11}(N) = \frac{\sigma_1 + 2\sigma_3}{9K} + \frac{\sigma_1 - \sigma_3}{3G_1} + \frac{\sigma_1 - \sigma_3}{3\eta_1}\left(\frac{N}{f}\right) + \frac{1}{3}\frac{\sigma_1 - \sigma_3}{G_2}\left\{1 - \exp\left[-\frac{G_2}{\eta_2}\left(\frac{N}{f}\right)\right]\right\} + \frac{1}{3}(\sigma_1 - \sigma_3 - \sigma_{\text{av}})\frac{1}{\eta_{30}n}\left(\frac{N}{f}\right)^n, \tag{30}$$

$$\varepsilon_{33}(N) = \frac{\sigma_1 + 2\sigma_3}{9K} + \frac{\sigma_3 - \sigma_1}{6G_1} + \frac{\sigma_3 - \sigma_1}{6\eta_1}\left(\frac{N}{f}\right) + \frac{\sigma_3 - \sigma_1}{6G_2}\left(\left\{1 - \exp\left[-\frac{G_2}{\eta_2}\left(\frac{N}{f}\right)\right]\right\}\right) - \frac{1}{3}(\sigma_1 - \sigma_3 - \sigma_{\text{av}})\frac{1}{\eta_{30}n}\left(\frac{N}{f}\right)^n. \tag{31}$$

5. Validation of NVPFM Adaptability

5.1. Parameter Determination and the Curve Fitting Method for Fatigue Constitutive Equations. For equations (28)–(31), the model parameters can be obtained by [48] regression analysis [49, 50]. 1stOpt is world's leading software for nonlinear curve fitting and the comprehensive optimization analysis of nonlinear equation parameters. It has been widely recognized in the field of nonlinear regression, nonlinear curve fitting, and parameter estimation of the nonlinear equation. The genetic algorithm (GA) method is a built-in nonlinear optimization control algorithm in 1stOpt, which can solve the parameter value of the multiparameter nonlinear equation and fit the nonlinear curve according to the corresponding data [45]. In this article, the GA method in

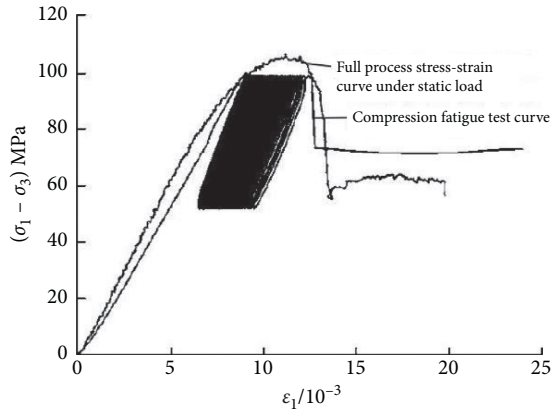

Figure 10: Fatigue curve and static curve of red sandstone under 15 MPa confining pressure [51].

Table 1: NVPFM parameters of red sandstone under 15 MPa confining pressure.

K (MPa)	G_1 (MPa)	G_2 (MPa)	η_1 (MPa·s)	η_2 (MPa·s)	η_{30} (MPa·s^n)	n	R^2
1.759×10^3	3.439×10^9	1.070×10^4	3.922×10^4	2.613×10^4	4.788×10^4	0.872	0.990

1stOpt was used to solve the parameters of the proposed model and fit the curve of test data.

The proposed three-dimensional NVPFM can describe the creep of the rock under cyclic loading. The parameters of the three-dimensional NVPFM equation can be solved. According to the previous study [42], the detailed process of obtaining model parameters and fitting test data is as follows. According to the stress condition of the sample during the test, when rocks undergo fatigue breakdown, equation (30) is selected. However, when rocks do not undergo fatigue breakdown, equation (28) is selected. Then, the test data from the literature and the selected constitutive equation were input into software in the form of a program. Afterwards, the GA method was used to fit the fatigue curve of the rock under cyclic loading. After the program runs, the parameter values and the curve of the model can be obtained. In this study, only the constitutive equation of the rock under fatigue breakdown is studied.

5.2. Verification of the Fatigue Model under Cyclic Loading

5.2.1. Model Parameters and the Curve of Red Sandstone. Zhang et al. [51] used sinusoidal wave cyclic loading with 0.2 Hz frequency to conduct triaxial tests on red sandstone under confining pressure. The fatigue curve of red sandstone under 15 MPa confining pressure is shown in Figure 10. It can be obtained that the static strength σ_c of red sandstone under 15 MPa confining pressure was 104.653 MPa, and its critical strength σ_s was 98.22 MPa by Origin software. The deviatoric stress acting on the RS-4-3 specimen under cyclic loading was in the range from 51.8 to 99.1 MPa. Constitutive equation (30) based on the proposed fatigue model was used to fit the fatigue curve of the RS-4-3 specimen. The obtained parameters and the curve of the NVPFM are shown in Table 1 and Figure 11, respectively.

5.2.2. Model Parameters and the Curve of the Water-Rich Soft Rock. In order to study the dynamic characteristics and structural safety of the soft rock in the foundation of the high-speed railway tunnel, Ding [52] used the MTS rock dynamic system to carry out fatigue tests on the water-rich soft rock under different dynamic stress ratios η_d (see equation (32)) by using the loading method shown in Figure 12. The effects of dynamic stress amplitude σ_d and static deviatoric stress σ_{st} on the fatigue characteristics of the water-rich soft rock were studied by Ding [52]. The critical stress ratio η_d of the water-rich soft rock under 200 kPa confining pressure, 180 kPa static deviatoric stress σ_{st}, 3 Hz loading frequency, and 50 kPa groundwater pressure is 0.3–0.5. In this paper, the critical dynamic stress ratio of the water-rich soft rock is 0.4, and the critical dynamic stress amplitude σ_{dc} is 240 kPa. The cyclic loading $\sigma_1(t)$ is expressed by equation (33). Then, the upper limit σ_{lmax} (34) of cyclic loading can be obtained from equation (33). The critical strength of the water-rich soft rock σ_s was $\sigma_{st} + (\sigma_{dc}/2)$. For the dynamic strength σ_c rock, Ge [53] found that the critical strength of the rock under confining pressure is 0.85 to 0.9 times of the static strength of the rock. Therefore, the static strength σ_c of the water-rich soft rock was taken as $\sigma_s/0.85$ in this study. The static strength σ_c of the water-rich soft rock under 200 kPa confining pressure was 353 kPa, and its critical strength σ_s was 300 kPa. Constitutive equation (28) based on the NVFPM proposed was used to fit the fatigue curve of the water-rich soft rock under cyclic loading with 300 kPa dynamic stress amplitude and dynamic stress ratio of 0.5. The fitting results and model parameters are shown in Table 2 and Figure 13.

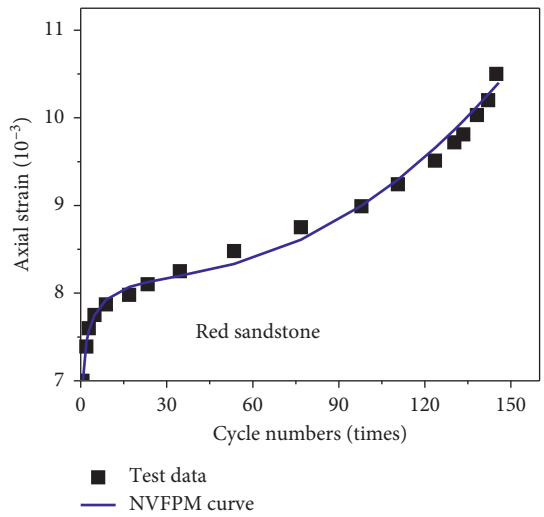

Figure 11: Fatigue deformation of red sandstone [51] fitted by the NVPFM.

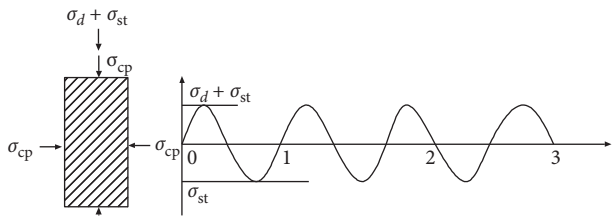

Figure 12: Stress state acting on the specimen and loading waveform [52].

Table 2: NVPFM parameters of the water-rich soft rock under 200 kPa confining pressure when η_d is 0.5.

K (kPa)	G_1 (kPa)	G_2 (kPa)	η_1 (kPa·s)	η_2 (kPa·s)	η_{30} (kPa·s^n)	n	R^2
5.830×10^4	6.899×10^7	1.320×10^4	3.037×10^7	2.023×10^5	1.7516×10^{16}	6.559	0.994

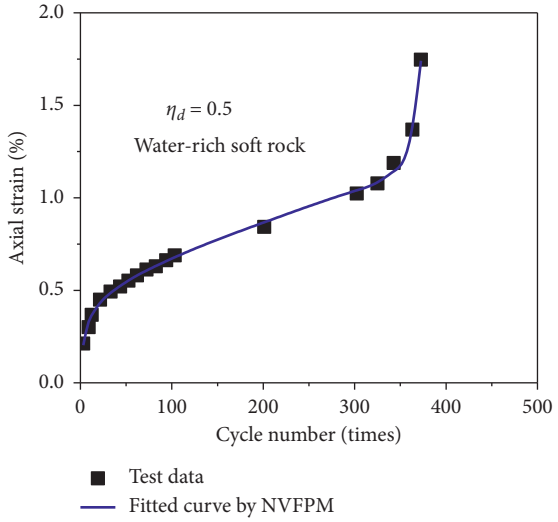

Figure 13: NVPFM curve of the water-rich soft [52] rock under 200 kPa confining pressure.

$$\eta_d = \frac{\sigma_d}{\sigma_{cua}}, \tag{32}$$

where σ_{cua} is the uniaxial compressive strength of the water-rich soft rock, and its value is 0.6 MPa.

$$\sigma_1(t) = \sigma_{cp} + \sigma_{st} + \left(\frac{\sigma_d}{2}\right)\sin(\omega t), \tag{33}$$

$$\sigma_{1\,max} = \sigma_{cp} + \sigma_{st} + \left(\frac{\sigma_d}{2}\right). \tag{34}$$

5.2.3. Model Parameters and the Curve of the Water-Rich Soft Rock When Fatigue Breakdown Does Not Occur. In order to analyze the effect of dynamic stress amplitude on creep characteristics of the water-rich soft rock, Ding [52] conducted comparative tests on rocks under cyclic loading with dynamic stress amplitudes of 30, 60, 90, 120, and 180 kPa, respectively. The corresponding dynamic stress ratios under the five working conditions were 0.05, 0.1, 0.15, 0.2, 0.3, and 0.5. During testing, the loading frequency of cyclic loading

Table 3: NVPFM parameters of the water-rich soft rock under 20 kPa confining pressure when η_d is 0.5.

η_d	$\sigma_1 - \sigma_3$ (kPa)	K (kPa)	G_1 (kPa)	G_2 (kPa)	η_1 (kPa·s)	η_2 (kPa·s)	R^2
0.05	73.744	-5.894×10^9	2.229×10^4	3.227×10^4	1.026×10^7	4.100×10^5	0.992
0.1	83.771	5.694×10^3	-2.259×10^3	2.070×10^4	3.808×10^6	1.634×10^5	0.999
0.15	95.160	2.780×10^4	-2.030×10^4	1.906×10^4	3.744×10^6	2.233×10^5	0.999
0.2	108.098	8.404×10^4	-2.643×10^8	1.417×10^4	4.463×10^6	2.078×10^4	0.997
0.3	232.273	6.493×10^4	-1.131×10^9	1.656×10^4	3.416×10^6	2.030×10^5	0.999

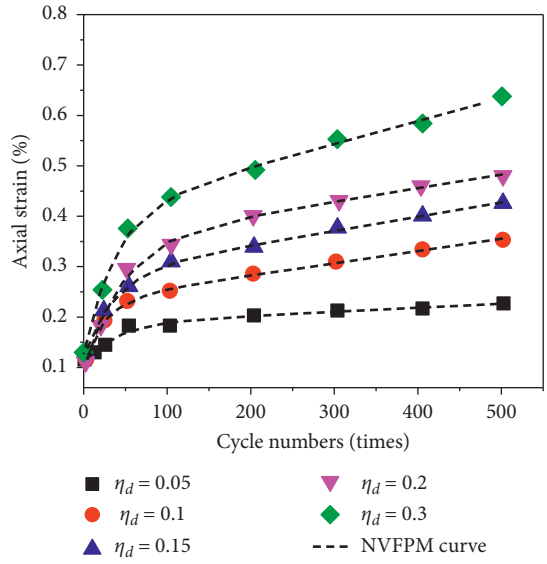

Figure 14: NVPFM curve of the water-rich soft rock [52] under 200 kPa confining pressure when fatigue breakdown does not occur.

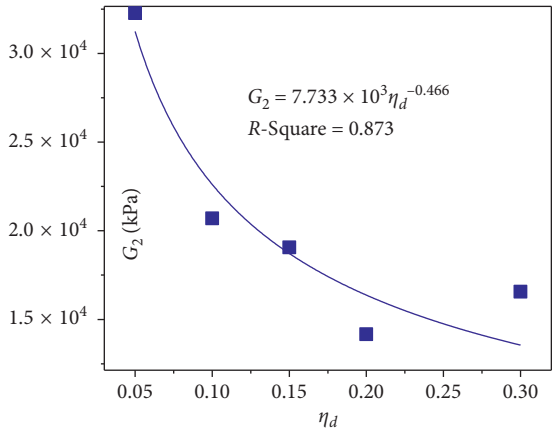

Figure 15: Relationship between G_2 and η_d.

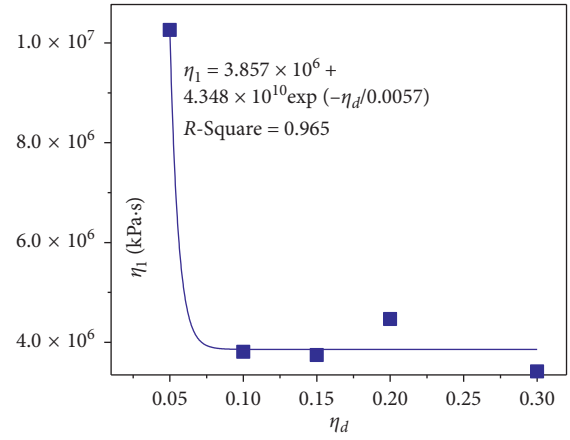

Figure 16: Relationship between η_1 and η_d.

was 3 Hz, the static deviatoric stress was 180 kPa, and the applied confining pressure was 200 kPa. From the data obtained from the test, the model parameters and model curves of the proposed fatigue constitutive equation (28) can be obtained. The obtained parameters and curves of the NVFPM are shown in Table 3 and Figure 14, respectively.

It can be seen from Figure 14 that fatigue constitutive equation (28) established in this paper can reflect the transient, steady-state, creep phases of rocks under cyclic loading. The correlation between model and test data was good. As can be seen from Table 3, when $\sigma_1 - \sigma_3 < \sigma_{av}$, the rock does not suffer from fatigue failure, and some of the obtained parameters of the model showed apparent regularity. The values of viscoelastic shear fatigue parameters G_2 and viscoelastic shear fatigue parameters η_1 decay exponentially with the increase in the dynamic strain ratio η_d. The specific attenuation law is shown in Figures 15 and 16. For the specific change of other parameters that cannot be determined for the time being, further study needs to be made in combination with more tests.

From the above regression analysis results, it can be seen that the fatigue constitutive model proposed in this paper can describe the creep characteristics of the rock under cyclic loading. When $(\sigma_1 - \sigma_3) \le \sigma_{av}$, rocks do not undergo fatigue breakdown, and the proposed model would degenerate into the burgers model, which can describe the transient, steady-state, and creep phases of the rock. When $(\sigma_1 - \sigma_3) \le \sigma_{av}$, rocks undergo fatigue breakdown, and the proposed NVPFM can reflect the transient, steady-state, and tertiary creep phases of the rock under cyclic loading.

6. Conclusions

According to the rheological mechanics, three-dimensional elastic, viscous, and plastic fatigue elements were constructed. Moreover, a fatigue yield criterion for the rock under cyclic loading was proposed based on the simplified cyclic loading in the previous study. A three-dimensional nonlinear visco-elastoplastic fatigue model (NFVPM) was established under confining pressure by using the flow rules

related to the proposed fatigue yield criterion. Finally, the rationality of the model is verified. The following conclusions can be drawn from this study.

The established NFVPM can describe the transient, steady-state, and tertiary creep phases of the rock under cyclic loading. Under confining pressure stress state, when the proposed fatigue yield criterion of the rock $F(J_2, \sigma_{av}) \leq 0$, the model degenerates into a burgers model that describes the transient and steady-state creep phases of the rock under cyclic loading. However, when $F(J_2, \sigma_{av}) > 0$ and the parameter $n \neq 1$, the model is a NFVPM that describes the transient, steady-state, and tertiary creep phases of the rock under cyclic loading.

The parameters of the NFVPM can be easily solved using mathematical methods. The parameters G_2 and η_1 of the NFVPM decreased with the increase in dynamic stress ratio η_d in the way of power function. Moreover, the curves of the NFVPM were in good agreement with the experimental results, and the correlation was above 0.990.

Data Availability

The data used to support the findings of this study are available within this article.

Conflicts of Interest

The authors declare that they have no conflicts of interest.

Acknowledgments

The authors would like to acknowledge the financial support from the National Natural Science Foundation of China (nos. 51968010 and 51608141), the Talents Scientific Research Foundation of Guizhou University (Grant no. (2015) 16), and National Science and Technology Support Plan for the 12th Five-Year Plan of China (no. 2011BAJ03B00).

References

[1] M. N. Bagde and V. Petroš, "Fatigue properties of intact sandstone samples subjected to dynamic uniaxial cyclical loading," *International Journal of Rock Mechanics and Mining Sciences*, vol. 42, no. 2, pp. 237–250, 2005.

[2] J. Lemaitre and J. L. Chaboche, *Mechanics of Solid Material*, Cambridge University Press, London, UK, 1990.

[3] C. D. Martin, P. K. Kaiser, and R. Christiansson, "Stress, instability and design of underground excavations," *International Journal of Rock Mechanics and Mining Sciences*, vol. 40, no. 7-8, pp. 1027–1047, 2003.

[4] D. Song, E. Wang, and J. Liu, "Relationship between EMR and dissipated energy of coal rock mass during cyclic loading process," *Safety Science*, vol. 50, no. 4, pp. 751–760, 2012.

[5] M. K. Duan, C. B. Jiang, H. L. Xing, D. M. Zhang, K. Peng, and W. Z. Zhang, "Study on damage of coal based on permeability and load-unload response ratio under tiered cyclic loading," *Arabian Journal of Geosciences*, vol. 13, no. 6, 2020.

[6] Y. Zhang, Z. Zhang, S. Xue, R. Wang, and M. Xiao, "Stability analysis of a typical landslide mass in the three gorges reservoir under varying reservoir water levels," *Environmental Earth Sciences*, vol. 79, no. 1, 2020.

[7] Ł. Wojtecki, M. J. Mendecki, W. M. Zuberek, and M. Knopik, "An attempt to determine the seismic moment tensor of tremors induced by destress blasting in a coal seam," *International Journal of Rock Mechanics and Mining Sciences*, vol. 83, pp. 162–169, 2016.

[8] C.-P. Lu, L.-M. Dou, N. Zhang et al., "Microseismic frequency-spectrum evolutionary rule of rockburst triggered by roof fall," *International Journal of Rock Mechanics and Mining Sciences*, vol. 64, pp. 6–16, 2013.

[9] B. G. Tarasov and M. F. Randolph, "Superbrittleness of rocks and earthquake activity," *International Journal of Rock Mechanics and Mining Sciences*, vol. 48, no. 6, pp. 888–898, 2011.

[10] R. Song, Y. Li, and J. W. Van de Lindt, "Loss estimation of steel buildings to earthquake mainshock-aftershock sequences," *Structural Safety*, vol. 61, pp. 1–11, 2016.

[11] C. Zhai, W. Wen, D. Ji, and S. Li, "The influences of aftershocks on the constant damage inelastic displacement ratio," *Soil Dynamics and Earthquake Engineering*, vol. 79, pp. 186–189, 2015.

[12] R. Han, Y. Li, and J. van de Lindt, "Impact of aftershocks and uncertainties on the seismic evaluation of non-ductile reinforced concrete frame buildings," *Engineering Structures*, vol. 100, pp. 149–163, 2015.

[13] S. Suresh, *Fatigue of Materials*, Cambridge University Press, Cambridge, UK, 1998.

[14] C. D. Martin and N. A. Chandler, "The progressive fracture of Lac du Bonnet granite," *International Journal of Rock Mechanics and Mining Sciences & Geomechanics Abstracts*, vol. 31, no. 6, pp. 643–659, 1994.

[15] E. Eberhardt, D. Stead, and B. Stimpson, "Quantifying progressive pre-peak brittle fracture damage in rock during uniaxial compression," *International Journal of Rock Mechanics and Mining Sciences*, vol. 36, no. 3, pp. 361–380, 1999.

[16] J. S. O. Lau and N. A. Chandler, "Innovative laboratory testing," *International Journal of Rock Mechanics and Mining Sciences*, vol. 41, no. 8, pp. 1427–1445, 2004.

[17] M. J. Heap, S. Vinciguerra, and P. G. Meredith, "The evolution of elastic moduli with increasing crack damage during cyclic stressing of a basalt from Mt. Etna volcano," *Tectonophysics*, vol. 471, no. 1-2, pp. 153–160, 2009.

[18] N. T. Burdine, "Rock failure under dynamic loading conditions," *Society of Petroleum Engineers Journal*, vol. 3, no. 1, pp. 1–8, 1963.

[19] H. R. Hardy Jr. and Y. P. Chugh, "Failure of geologic materials under low-cycle fatigue," in *Proceedings of the 6th Canadian Symposium on Rock Mechanics*, pp. 33–47, Montreal, Canada, 1970.

[20] K. Suzuki, Y. Nishimatsu, and R. Heroesewojo, "The statistical distribution of fatigue life and the S-N curve of rocks," *Journal of the Mining Institute of Japan*, vol. 86, no. 986, pp. 353–358, 1970.

[21] L. S. Costin and D. J. Holcomb, "Time-dependent failure of rock under cyclic loading," *Tectonophysics*, vol. 79, no. 3-4, pp. 279–296, 1981.

[22] Z. Y. Tao and M. H. Mo, "An experimental study and analysis of the behaviour of rock under cyclic loading," *International Journal of Rock Mechanics and Mining Sciences & Geomechanics Abstracts*, vol. 27, no. 1, pp. 51–56, 1990.

[23] T. N. Singh, S. K. Ray, and D. P. Singh, "Effect of uniaxial cyclic compression on the mechanical behaviour of rocks," *Indian Journal of Engineering and Materials Sciences*, vol. 1, pp. 118–120, 1994.

[24] S. K. Ray, M. Sarkar, and T. N. Singh, "Effect of cyclic loading and strain rate on the mechanical behaviour of sandstone,"

International Journal of Rock Mechanics and Mining Sciences, vol. 36, no. 4, pp. 543–549, 1999.

[25] J.-I. Kodama, Y. Ishizuka, T. Abe, Y. Ishijima, and T. Goto, "Estimation of the fatigue strength of granite subjected to long-period cyclic loading," *Shigen-to-Sozai*, vol. 116, no. 2, pp. 111–118, 2000.

[26] M. N. Bagde and V. Petroš, "Fatigue and dynamic energy behavior of rock subjected to cyclical loading," *International Journal of Rock Mechanics and Mining Sciences*, vol. 46, no. 1, pp. 200–209, 2009.

[27] B. Huang and J. Liu, "The effect of loading rate on the behavior of samples composed of coal and rock," *International Journal of Rock Mechanics and Mining Sciences*, vol. 61, pp. 23–30, 2013.

[28] K. Arora, T. Chakraborty, and K. S. Rao, "Experimental study on stiffness degradation of rock under uniaxial cyclic sinusoidal compression loading," *Rock Mechanics and Rock Engineering*, vol. 52, no. 11, pp. 4785–4797, 2019.

[29] P. G. Kang, J. Q. Zhou, Q. L. Zou, and X. Song, "Effect of loading frequency on the deformation behaviours of sandstones subjected to cyclic loads and its underlying mechanism," *International Journal of Fatigue*, vol. 131, Article ID 105349, 2020.

[30] K. Fuenkajorn and D. Phueakphum, "Effects of cyclic loading on mechanical properties of maha sarakham salt," *Engineering Geology*, vol. 112, no. 1–4, pp. 43–52, 2010.

[31] B. C. Haimson and C. M. Kim, "Mechanical behavior of rock under cyclic fatigue," in *Proceedings of thirteenth Symposium on Rock Mechanics*, pp. 845–863, Urbana, IL, USA, 1972.

[32] B. C. Haimson, "Effect of cyclic loading on rock," *Dynamic Geotechnical Testing*, pp. 228–245, ASTM STP654, Philadelphia, PA, USA, 1978.

[33] J. Kodama, Y. Ishizuka, T. Abe, and Y. Ishijima, "Fatigue, creep properties and long-term strength of granite under uniaxial compression," *Shigen-to-Sozai*, vol. 108, no. 3, pp. 182–186, 1992.

[34] Y. ..J. Yang, Y. Song, and J. Chu, "Experimental study on characteristics of strength and deformation of coal under cyclic loading," *Chinese Journal of Rock Mechanics and Engineering*, vol. 26, no. 1, pp. 201–204, 2007, in Chinese.

[35] J.-Q. Xiao, D.-X. Ding, F.-L. Jiang, and G. Xu, "Fatigue damage variable and evolution of rock subjected to cyclic loading," *International Journal of Rock Mechanics and Mining Sciences*, vol. 47, no. 3, pp. 461–468, 2010.

[36] J.-Q. Xiao, D.-X. Ding, G. Xu, and F.-L. Jiang, "Inverted S-shaped model for nonlinear fatigue damage of rock," *International Journal of Rock Mechanics and Mining Sciences*, vol. 46, no. 3, pp. 643–648, 2009.

[37] H. Y. Liu, S. R. Lv, L. M. Zhang, and X. P. Yuan, "A dynamic damage constitutive model for a rock mass with persistent joints," *International Journal of Rock Mechanics and Mining Sciences*, vol. 75, pp. 132–139, 2015.

[38] N. Li, W. Chen, P. Zhang, and G. Swoboda, "The mechanical properties and a fatigue-damage model for jointed rock masses subjected to dynamic cyclical loading," *International Journal of Rock Mechanics and Mining Sciences*, vol. 38, no. 7, pp. 1071–1079, 2001.

[39] B. Y. Zhao, T. Z. Huang, D. Y. Liu, D. S. Liu, Y. Liu, and X. P. Wang, "Experimental study and damage model study of rock salt subjected to cyclic loading and cyclic creep," *Advances in Civil Engineering*, vol. 2020, Article ID 8049626, 11 pages, 2020.

[40] Z. C. Wang, J. G. Zhao, S. C. Li, Y. G. Xue, Q. S. Zhang, and Y. Y. Jiang, "Fatigue mechanical behavior of granite subjected to cyclic loading and its constitutive model," *Chinese Journal of Rock Mechanics and Engineering*, vol. 13, no. 3, pp. 1188–1900, 2012, in Chinese.

[41] J. B. Wang, X. R. Liu, M. Huang, and X. Yang, "Analysis of axial creep properties of salt rock under low frequency cyclic loading using burgers model," *Rock and Soil Mechanics*, vol. 35, no. 4, pp. 934–941, 2014, in Chinese.

[42] J. Q. Guo and Z. H. Huang, "Constitutive model for fatigue of rock under cyclic loading," *Chinese Journal of Geotechnical Engineering*, vol. 37, no. 9, pp. 1698–1703, 2015, in Chinese.

[43] S. Y. Pu, Z. D. Zhu, L. Song, W. L. song, and Y. Y. Peng, "Fractional-order visco-elastoplastic constitutive model for rock under cyclic loading," *Arabian Journal of Geosciences*, vol. 13, no. 9, p. 326, 2020.

[44] Y. Liu, F. Dai, L. Dong, N. Xu, and P. Feng, "Experimental investigation on the fatigue mechanical properties of intermittently jointed rock models under cyclic uniaxial compression with different loading parameters," *Rock Mechanics & Rock Engineering*, vol. 51, no. 1, pp. 47–68, 2017.

[45] A. Momeni, M. Karakus, G. R. Khanlari, and M. Heidari, "Effects of cyclic loading on the mechanical properties of a granite," *International Journal of Rock Mechanics and Mining Sciences*, vol. 77, pp. 89–96, 2015.

[46] H. Q. Liu, S. Y. Pu, X. J. Liu, Q. Li, Z. C. Hao, L. Li et al., "Fractional-order visco-elasto-plastic constitutive model for rock under cyclic loading," *Journal of Yangtze River Scientific Research Institute*, vol. 35, no. 9, pp. 127–132, 2018.

[47] H. Schiessel, R. Metzler, A. Blumen, and T. F. Nonnenmacher, "Generalized viscoelastic models: their fractional equations with solutions," *Journal of Physics A: Mathematical and General*, vol. 28, no. 23, pp. 6567–6584, 1995.

[48] J. Sun, *Rheological Behavior of Geomaterials and its Engineering Application*, Architecture and Building Press, Beijing, China, 1999, in Chinese.

[49] K. Fuenkajorn and S. Serata, "Geohydrological integrity of CAES in rock salt," in *Proceedings of the 2nd International Conference on Compressed-Air Energy Storage*, Electric Power Research Institute, San Francisco, CA, USA, pp. 4.1–4.21, 1992.

[50] S. Serata and K. Fuenkajorn, "Formulation of a constitutive equation for salt," in *Proceedings of the Seventh International Symposium on Salt*, Elsevier Science Publishers, Kyoto, Japan, pp. 483–488, 1992.

[51] Q. X. Zhang, X. R. Ge, M. Huang, and H. Sun, "Testing study on fatigue deformation law of red-sandstone under triaxial compression with cyclic loading," *Chinese Journal of Rock Mechanics and Engineering*, vol. 25, no. 3, pp. 474–478, 2006.

[52] Z. D. Ding, "Dynamic properties of soft rock and the safety of base structure of high-speed railway tunnels," Dissertation, Central South University, Hunan, China, 2012, in Chinese.

[53] X. R. Ge, "Study on deformation and strength behaviour of the large-sized triaxial rock samples under cyclic loading," *Rock and Soil Mechanics*, vol. 8, no. 2, pp. 11–19, 1987, in Chinese.